

# Spreading Depression in Focal Ischemia: A Computational Study

February 27, 1997

Kenneth Revett\*, Eytan Ruppin<sup>†</sup>, Sharon Goodall \*, and James A. Reggia\*

## Correspondence:

Dr. James A. Reggia  
Dept. of Neurology  
University of Maryland Hospital  
22 S. Greene St.  
Baltimore, MD 21201

Phone: (301) 405-2686  
Fax: (301) 405-6707  
E-mail: reggia@cs.umd.edu

\* Depts. of Neurology and Computer Science, Inst. for Adv. Comp. Studies, University of Maryland

<sup>†</sup> Dept. of Computer Science and Physiology, Tel Aviv University

This manuscript contains: 36 pages, 6 Figures and 3 Tables.

Word count: Abstract: 177, Introduction: 500, Discussion: 1100

**Acknowledgment:** Supported by NINDS Award NS29414, Israeli Ministry of Health Grant No. 01350931, and by an Alon Fellowship to Dr. Ruppin.

## Abstract

When an ischemic cerebral infarction occurs, surrounding the core of dying tissue there is usually an *ischemic penumbra* of non-functional but still viable tissue. One current but controversial hypothesis is that this penumbra tissue often eventually dies due to the metabolic stress imposed by multiple cortical spreading depression (CSD) waves, i.e., by ischemic depolarizations. We describe here a computational model of CSD developed to study the implications of this hypothesis. Following simulated infarction, the model displays the linear relationship between final infarct size and the number of CSD waves traversing the penumbra that has been reported experimentally, even though damage with each individual wave progresses non-linearly with time. It successfully reproduces the experimental dependency of final infarct size on mid-penumbra cerebral blood flow and potassium reuptake rates, and identifies a critical penumbra blood flow rate beyond which damage does not occur. The model makes testable predictions about the number, velocity and duration of ischemic CSD waves. These findings support the hypothesis that CSD waves play an important causal role in the death of ischemic penumbra tissue.

**Keywords:** *focal ischemia, cortical spreading depression, computational models, stroke, ischemic penumbra and post-infarct debilitation.*

Running title: *A Computational Model of Spreading Depression*

Understanding the mechanisms underlying tissue damage in the ischemic penumbra is of paramount clinical importance, as it may lead to new therapeutic measures that reduce post-infarct debilitation. While great progress has been made in this area during recent years (Iijima *et al.*, 1992; Mies *et al.*, 1993; Choi, 1994; Fisher & Garcia, 1996), the mechanisms by which focal ischemia evolves into infarction and the factors which determine the ultimate extent of the infarct are still unsettled. The prolonged reduction of blood supply in the peri-infarct region may gradually lead to progressive tissue damage via numerous pathological metabolic pathways, yet the relative importance of these factors remains controversial (Pulsinelli, 1992; Hossman, 1994a; Hossmann, 1994b; Heiss & Graf, 1994). In this paper, we develop and study the first computational model of the ischemic penumbra to examine one of the main mechanisms hypothesized to be causally linked to penumbra tissue death: *cortical spreading depression (CSD) waves*.

Cortical spreading depression (CSD) is a wave of reduced spontaneous electrical activity and biochemical changes that spreads across the normal cerebral cortex at a rate of about 2 – 5 mm/min. It is characterized by transient reductions in EEG power, failure of neurons to respond to evoked potentials, negative extracellular DC potential shifts, and increased extracellular potassium and L-glutamate (Nedergaard & Hansen, 1993). Very similar, repetitive spreading depression waves, called ischemic depolarizations, have also been reported to originate from the core of an infarct and progress outwards into the penumbra. Such waves have been recorded in various animal models of ischemia by numerous laboratories (Nedergaard & Astrup, 1986; Gill *et al.*, 1992; Iijima *et al.*, 1992; Mies *et al.*, 1993; Back *et al.*, 1994; Heiss & Graf, 1994; Hossman, 1994a).

Under normoxic conditions, CSD waves do not appear to generate any morphologically detectable damage; this is not true under hypoxic/ischemic conditions, where varying degrees of damage occurs (Nedergaard & Hansen, 1988). The movement of CSD waves across the cortex may be viewed as a reaction-diffusion process (Lauritzen, 1994). The reaction component supplies  $K^+$  from cells that have been necrotized (ischemic tissue), and from intracellular  $K^+$  released by depolarization when the extracellular levels of  $K^+$  increase above some threshold (intact tissue). The released  $K^+$  moves by diffusion out from the source in a radial fashion. Neurons and glial cells respond physiologically by increasing their Na/K-ATPase activity which in turn reduces the levels of extracellular  $K^+$ . If the cells are compromised metabolically, this energy expenditure can deplete the energy reserves of the cell, generating a transient mismatch between energy supplies and demand, resulting in transient episodes of tissue hypoxia and lactic acidosis (Mayevsky *et al.*, 1982;

Mayevsky & Weiss, 1991; Back *et al.*, 1994; Gyngell *et al.*, 1994). The ensuing gradual depletion of tissue ATP and high energy phosphate reserves following repetitive CSD waves may eventually lead to peri-infarct tissue death, depending on their frequency and duration (Takagi *et al.*, 1993; Gyngell *et al.*, 1994).

Several studies in experimental animal models of stroke have suggested a significant correlation between the number of CSD waves and the evolving infarct volume (Gill *et al.*, 1992; Iijima *et al.*, 1992; Chen *et al.*, 1993; Mies *et al.*, 1993; Back *et al.*, 1996). However, even in light of recent diffusion mapping studies showing an increase in infarct volume associated with CSD waves, the causative role of CSD waves in the evolution of penumbra damage still remains uncertain (Takano *et al.*, 1996). In this paper we study the CSD hypothesis in stroke with the aid of a computational model. After verifying the model's consistency with experimental data, we investigate systematically how various physiological parameters interact and influence the ultimate amount of tissue damage. The results provide support for the CSD hypothesis in stroke, and the model makes testable predictions meriting further experimental investigation.

## 1 Methods

Models of ionic changes in CSD in normoxic tissue have been developed in the past, but these models were either one dimensional, or two dimensional with limited metabolic/physiological scope (Tuckwell & Miura, 1978; Reshodko & Bures, 1975). Recently, a simple two dimensional model of the ionic changes during CSD waves in normoxic tissue and during migraine aura has been developed (Reggia & Montgomery, 1996). The basic core of the model presented in this paper draws upon this recent normoxic CSD modeling study, but it has been further developed and extensively expanded to capture the important descriptors of CSD waves in the realm of acute focal stroke.

In our model, we express the relations and interactions between the main variables of interest as a set of coupled differential equations. Solving these equations enables one to trace the model's evolution in time, given initial conditions and parameter settings. This formal model was then implemented as a computer program, transforming the differential equations into a set of difference equations which are solved by numerical integration.

The main problems one encounters when trying to study complex biological events like ischemic stroke computationally is the richness of these models and the incompleteness of relevant quantita-

tive data. The large number of variables involved and their intricate and non-linear dependencies pose a tremendous barrier. These problems are further augmented by implementation issues. As a model becomes increasingly realistic, more computational resources are required, and the difficulty of visualizing the multi-dimensional information in order to interpret the model's behavior also increases dramatically. As a result, as we have done in this work, one needs to focus on a subset of key variables, and to determine convenient ways of tracing their temporal and spatial evolution. Below we provide an overview of the mathematical model, its computational implementation, and experimental methods. A detailed technical description of the model is given in the Appendix.

## 1.1 The Model

The model has been constructed according to two main guiding principles: to incorporate a causative role of CSD waves in the progression of peri-infarct damage, and to faithfully capture the basic characteristics of CSD waves in normoxic and ischemic tissue. The first guideline has determined the general structure of the model, i.e., its main variables and their mutual interactions; the model is specifically designed such that the propagation of CSD waves through penumbra tissue with impaired blood supply can cause an accumulative metabolic energy shortage, which may lead to progressive tissue damage. The second principle has mainly guided the choice of the model parameters, i.e., the strength of the interactions between the different model variables.

The model is based on a multi-dimensional set of non-linear differential equations that govern the temporal evolution of several key metabolic variables involved in CSD waves (listed in the Appendix). Both the spatial structure of the cerebral cortex and time are discretized. The cortex is represented as a two-dimensional array of elements, each of which represents a small volume of cortex. One cortical element is 0.125 mm in length, and one time step corresponds to 13 msec. As elaborated below, each cortical element  $i$  has its own value for extracellular potassium  $K_i$ , reuptake  $R_i$ , metabolic stores  $M_i$ , persistent impairment  $P_i$ , tissue intactness  $I_i$ , internal potassium stores  $S_i$ , and cerebral blood flow  $F_i$ . All variables incorporated into the model are dimensionless and are calculated and presented on a scaled basis from 0 to 1, as quantitative data on the rates of change for many of the variables in the model is unavailable.

The rate of change of *extracellular potassium concentration* ( $K_i$ ) is modeled as a reaction-diffusion process governed by four terms: 1. A diffusion term which reflects the passive movement of potassium ions along their spatial concentration gradient (in two dimensions); 2. A reaction term

which models the regenerative processes that generate the sharp rise of extracellular potassium concentration occurring when  $K_i$  values exceed a threshold level and generate CSD waves; 3. A reuptake term which represents the reuptake of extracellular potassium by neuronal and glial Na/K-ATPase pumps; and 4. An infusion term - reflecting either an external source of potassium infusion (in experiments simulating CSD wave generation in normoxic tissue) or intracellular potassium release to the extracellular space as a result of breakdown of neuronal membranes in dying ischemic tissue.

Two terms affect the rate of *potassium reuptake*,  $R_i$ , reflecting the functioning of the Na/K-ATPase pumps: a rate-increasing term proportional to the levels of extracellular potassium, tissue intactness and metabolic stores levels, and a decay term which brings Na/K-ATPase activity back to its resting level when  $K_i$  values are restored. The subset of the model incorporating the variables  $K_i$  and  $R_i$  is in part inspired by previous mathematical models of wave-like phenomena, such as calcium activation waves on the enclosing membranes of amphibian eggs (Cheer *et al.*, 1987; Lane *et al.*, 1987) and the FitzHugh-Nagumo model of action potentials in neurons (FitzHugh, 1961; Nagumo *et al.*, 1962). In undamaged, fully intact cortical tissue,  $K_i$  and  $R_i$  effectively reduce to the complete normoxic, non-ischemic CSD model we have already studied (Reggia & Montgomery, 1996).

The *metabolic stores level* ( $M_i$ ) determines the rate at which metabolic energy stores (glucose and high energy phosphates, grouped together in a single variable) are generated. The level of these stores at each volume element is determined by competition between supply and demand terms. The supply term is proportional to the blood flow rate, tissue intactness and current energy level stores. The demand term, representing cerebral metabolic consumption rates, includes a basal metabolic rate term and is also proportional to the reuptake rate.

The *cerebral blood flow* of a given cortical unit ( $F_i$ ) is modulated by that unit's metabolic stores and current level of cerebral blood flow. The magnitude of the hemodynamic response in simulated focal ischemia is determined by the location of the cortical unit along the penumbra. For instance, a cortical element located more proximal to the lesion core than another (and hence receiving less blood supply) will exhibit a reduced hemodynamic response to an equal metabolic demand.

The level of *tissue intactness* of a given cortical element ( $I_i$ ), identifies the fraction of cellular components in that element which remain undamaged (tissue damage is assumed to be irreversible). Tissue damage occurs in a cumulative fashion whenever the energy stores of a cortical element fall

below a threshold value, and the extent of the damage is proportional to the extent and duration the energy stores are below the intactness threshold (damage is continuous on a scale of 0 to 1). This threshold value ( $P_{\Theta}$ ) is not fixed and is itself modulated by  $P_i$ , the partial impairment, a variable which denotes the susceptibility to damage for a given cortical element,  $i$ . The extent of the partial impairment,  $P_i$ , is proportional to the extent and duration of the cortical element's drop in metabolic stores below the partial impairment threshold,  $M_{\Theta}$ . The value of  $P_i$ , combined with the initial intactness threshold ( $P_{\Theta} + P_i$ ) determines the actual intactness threshold for a given cortical unit. This partial impairment formulation encompasses the increasing susceptibility of cortical tissue to the metabolic deficits that occur as a result of bouts of transient ischemia/hypoxia (Mies *et al.*, 1991; Iijima *et al.*, 1992). These metabolic deficits include such factors as an increase in free radicals, lactate acidosis and increased levels of intracellular  $Ca^{2+}$  concentrations. Finally, the level of *intracellular potassium stores* ( $S_i$ ) modulates the rate of potassium effusion from damaged tissue to the extracellular space. These stores fall exponentially when a cortical element is infarcted and  $K^+$  is released to the extracellular space.

## 1.2 Implementation

The formal model described above and in detail in the Appendix has been implemented as a C program that runs under Unix. A typical, single simulation takes about 2 hours when run on a contemporary engineering workstation (a DEC Alpha). An Euler numerical integration method is used, and key results have been verified using a fourth order Runge-Kutta method.

The model we present simulates both normoxic and ischemic CSD waves which occur in the cerebral cortex of a variety of experimental animals under anesthetic conditions. In all simulations, the cerebral cortex is represented as a two dimensional sheet of cortical elements (without modeling individual cellular components), each 0.125 mm wide, arranged in a hexagonal tessellation. The size of the two-dimensional array used in this paper is 150 x 150 elements (1.875 cm per dimension). The results presented are similar whether sealed-end or leakage boundary conditions were used. A single time step in the simulation corresponds to 13 milliseconds of real-time.

Two kinds of numerical experiments were performed: normoxic and ischemic simulations of CSD waves. In the *normoxic case*, CSD waves were generated by simulating infusion of potassium (by setting  $K_{inf}$  to a positive value in Eq. 1, Appendix) into the center of the model cortical region. In the *ischemic case*, the blood flow to the initial lesion core at the center of the model cortex is

clamped to zero for a simulated time period of a few hours and a penumbra gradient of cerebral blood flow was simulated. Cerebral blood flow was linearly graded from zero at the cortical element immediately adjacent to the lesion core, to the normal “resting value” at the outermost elements of the penumbra.

Part of the difficulties in studying a complex multi-variable model of the kind described here resides in tracing and visualizing the behavior of such a complex model. To this end, we employed two main visualization tools in this work. First, simulated multi-variable ‘probes’ are placed in specific locations in the cortex to trace the values of the various model variables as a function of time. The values of these variables are typically recorded at three distinct sites on the simulated cortex: the center of the lesion, 2.375 mm away from the center of the initial lesion core (half way across the penumbra), and in an intact region, 5.75 mm from the initial lesion core (or the center of the  $K^+$  stimulus in the normoxic simulations). Second, we generated two dimensional maps of the values of specific variables on the simulated cortex at a given moment. These maps can be displayed in a consecutive manner, providing an animated trace of the temporal evolution of these variables. In addition, some global quantities have been traced, such as the cumulative amount of tissue damage and the number of propagating CSD waves. Lastly, the physical characteristics of the CSD waves are automatically recorded by the simulation (e.g., wave duration and speed). The software required to run all of the simulations described in this paper is located at the <http://www.cs.umd.edu/~goodall/download.html> website.

## 2 Results

In this section we present the basic results of simulating both normoxic and ischemic CSD waves. The effects of varying the area of the initial lesion or the width of the penumbra, the effect of changing cerebral blood flow on final total infarct size, the relationship between the potassium reuptake rate and tissue damage, and the relationship between the number of CSD waves and final infarct area, are described. Lastly, the results of exploring the parameter space are discussed.

### 2.1 The Normoxic Case

The normoxic simulation produces CSD waves similar to those that have been reported to occur under conditions of normal cerebral blood flow in the cortex of a variety of experimental animals. The model equations and parameter values were selected via an extensive empirical trial-and-error

search process so that the model successfully reproduces the fundamental properties of normoxic CSD waves, their velocity and duration, and the accompanying negligible damage.

In the normoxic CSD simulations, a sufficient amount of  $K^+$  was infused into an area 2.5 mm wide ( $5.17 \text{ mm}^2$ , equivalent to the initial lesion core area in the ischemic simulations) located in the center of the simulated cortex such that at least one CSD wave is generated per infusion. The infusion regimen consists of 5 minute  $K^+$  pulses, repeated every 20 minutes. The values of the parameters and initial conditions used for the normoxic simulation can be found in Table 3 in the Appendix. Each potassium infusion pulse results in one CSD wave that propagates from the edge of the infusion area across the entire simulated cortex. CSD waves in the simulation traversed the cortex at a velocity of approximately 4.7 mm/min; consistent with the literature reports of normoxic CSD wave velocity of 2–5 mm/min (Hansen *et al.*, 1980; Nedergaard & Hansen, 1993). The duration of the normoxic CSD waves (approximately 80 seconds) is also consistent with literature reports (Nedergaard & Hansen, 1993; Sugaya *et al.*, 1975). No infarction was detected as a result of the CSD waves generated during 3 hours of intermittent infusion of potassium (data not shown).

*Figure 1 goes here*

Figure 1 presents the temporal behavior of the model variables during the passage of six normoxic CSD waves, as measured by a simulated electrode located 5.75 mm from the center of potassium infusion. Initially, the extracellular potassium levels are set to the normal resting level of 0.03 (corresponding to 3 mM). The external infusion of potassium elevates extracellular potassium above resting levels. When extracellular potassium levels exceed the auto-catalytic threshold value ( $K_{\Theta}$ ), potassium levels increase very rapidly to more than 20 times their resting levels. The reuptake variable rate ( $R$  in Figure 1) increases in response to rising extracellular potassium. As the reuptake mechanism returns the extracellular potassium levels back to basal levels, there is an initial undershoot of extracellular potassium followed by a slow return to resting levels. In the model, the length of time that extracellular potassium remains below resting levels determines the refractory period during which subsequent CSD waves cannot be generated (approximately 3 to 4 minutes in the model). The behavior of the reuptake variable also reveals a profile which has been reported for metabolic, energy-driven cellular processes (Hansen & Mutch, 1984). We equate the reuptake rate variable with the activity of the membrane bound Na/K-ATPase (of neuronal and/or glial origin).

Increased reuptake rate in response to high extracellular potassium levels reduces metabolic energy stores (ATP, ADP, AMP, phosphocreatine) by about 40% for all cortical elements invaded by the CSD wave ( $M$  in Figure 1), consistent with literature reports (Mies & Paschen, 1984; Gault *et al.*, 1994). As the tissue repolarizes, the metabolic energy stores return to basal levels within 5 minutes. There are numerous reports of the coupling between metabolic stores and cerebral blood flow under normoxic conditions (Mies & Paschen, 1984; Pulsinelli, 1992; Nedergaard & Hansen, 1993), which is also captured in the model. As demonstrated in Figure 1, the restoration of metabolic stores occurs concurrently with an increase in cerebral blood flow ( $F$  in Figure 1), with a value of 0.5 representing normal cerebral blood flow value in the model. In correspondence with the experimental literature, cerebral blood flow increases significantly in response to increased energy demands (up to 90%) and returns to basal levels shortly after the restoration of metabolic stores (Hansen *et al.*, 1980; Mies & Paschen, 1984; Back *et al.*, 1994; Zhang *et al.*, 1994). The other variables defined in the model: tissue intactness (I), partial impairment (P) and internal potassium stores (S), maintain their initial values in the normoxic simulation and are therefore not presented in Figure 1.

## 2.2 The Ischemic Case

In order to simulate focal ischemia within the model, cerebral blood flow is clamped to zero within an area designated as the initial lesion core and a cerebral blood flow gradient is established which defines the penumbra that surrounds the lesion. The parameters for the ischemic simulations are identical to those used in the normoxic model (except for the creation of a penumbra and the resulting gradient in resting metabolic stores that the penumbra generates). Figure 2 presents the temporal events as an infarct develops in the model, and shows how tissue damage gradually spreads as a result of the generation of CSD waves. Figure 2a presents a recording from the central cortical element within the ischemic core. Tissue intactness  $I$ , representing the percentage of viable cells within a cortical element, begins to decrease when the metabolic stores  $M$  fall below the intactness threshold. The metabolic stores decline as a result of the constant drain of basal metabolic consumption which is not sufficiently compensated for by cerebral blood flow. As intactness drops, extracellular potassium levels rises due to leakage from the internal stores of the affected cortical elements. Potassium reuptake, which requires metabolic energy, is negligible in the infarct core because of the reduced metabolic energy stores. With an initial lesion width of 2.5

mm, the core itself contributes  $5.17 \text{ mm}^2$  to the total damage. Any additional damage therefore occurs in the surrounding penumbra.

*Figure 2 goes here*

In addition to the intactness threshold, the model includes a partial impairment variable that captures the *cumulative* effect that metabolic drain has on the viability of the tissue. The effective intactness threshold is raised as metabolic stores drop below the partial impairment threshold, which in turn increases the probability that subsequent CSD waves will cause tissue damage at this location. In addition, the reuptake rate and the level of metabolic stores is decreased in direct proportion to the increase in the partial impairment term. Hence, processes that express a growing liability for damage, such as an increased intactness threshold and reduced energy production, occur concomitantly with processes that act to protect the tissue from further damage, such as decreased potassium reuptake (Hossman, 1994a).

Figure 2b presents the output of the same simulation recorded near the midpenumbra (approximately 2.4 mm from the center of the initial lesion) location. Five CSD waves were recorded outside the penumbra during this specific simulation. At midpenumbra, the fourth and fifth waves coalesced. The CSD waves exhibit the same basic profile found in normoxic simulations. The velocity of the CSD waves remained similar to that found in the normoxic simulations, although there was a trend towards a decrease (from 4.8 to 4.2 mm/min). Their duration exhibited a 28 % increase (from 2.5 to 3.2 mm/min) between the first and last wave (measured at the same location). The increase in CSD wave duration over time is consistent with experimental literature reports (Hansen & Mutch, 1984; Nedergaard & Astrup, 1986; Nedergaard & Hansen, 1993; Back *et al.*, 1995). The increase in CSD wave duration can be explained by the model as the result of the increase in the partial impairment term, which decreases the reuptake rate and the rate of metabolic stores production. Since these variables are required for the restoration of ionic homeostasis, any reduction in the magnitude of these variables will prolong the CSD wave duration. The cerebral blood flow  $F$  rises by 55% during the first wave in response to the decrease in  $M$ , which dropped by 62%. With each passing wave, the drop in  $M$  increases, without a proportional increase in  $F$ . In the model, tissue damage following the passage of a CSD wave occurs in the ischemic case and not in the normoxic case because of the reduction in cerebral blood flow and compromised hemodynamic response of tissue under ischemic conditions. The rise in cerebral blood flow is insufficient

to maintain metabolic stores above the partial impairment threshold.

### 2.3 Effects of Number of Waves, Lesion Size and Penumbra Size

Several simulations were done to examine the relationship between the number of waves passing through the penumbra and the total infarct area. In these simulations the gradient of blood flow supply was identical, and the number of waves generated in each simulation was varied by modifying three parameter values ( $c_{MR}$ ,  $c_{RR}$  and  $P_{\Theta}$ ). Figure 3a plots the infarct area over time (since the model is two-dimensional, we refer to infarct area as opposed to infarct volume) *as it evolves* during four simulations with a variable number of waves (2–5). The number of CSD waves versus the *final* infarct area is plotted in Figure 3b. These results shed light on an important apparent contradiction in the literature. On the one hand, it has been reported that there is a very strong linear correlation between the number of CSD waves and the size of the final infarct (Mies *et al.*, 1993). But on the other hand, using diffusion weighted imaging to map out damage as it occurs over time, it was recently shown that the infarct volume progresses in a less than linear fashion (Reith *et al.*, 1995; Takano *et al.*, 1996). Our model captures both the linear relation between the number of waves and the final infarct area (across experiments,  $r=0.992$ ) as shown in Figure 3b, as well as the non-linear relationship between the number of waves and the amount of evolving damage (in a given simulation). The pattern of infarct progression which is coupled to the passage of CSD waves is consistent with several recent reports that provide support for the hypothesis that CSD waves increase the infarct volume resulting from ischemic stroke (Mies *et al.*, 1993; Back *et al.*, 1996; Takano *et al.*, 1996).

*Figure 3 goes here*

We also investigated the effects of penumbra and initial lesion sizes on the number of CSD waves generated and the size of the final infarct. Figure 4a plots the effect of varying the initial lesion core area while holding the total area of ischemia (initial lesion core plus penumbra) constant. The relationship between initial lesion core area and final infarct area is roughly linear and highly correlated ( $r=0.973$ ). In addition, the number of CSD waves was reduced (data not shown) with an increase in the size of the initial core lesion (from a maximum of 4 to a minimum of 2 CSD waves). Figure 4b plots the final infarct size as a function of the width of the penumbra (holding the initial lesion core area fixed), showing a positive linear relationship ( $r=0.988$ ). As the penumbra

size increased, the number of CSD waves increased (data not shown) from a minimum of 2 to a maximum of 7 CSD waves. Analyzing the model data, it became evident that in all simulations the infarct area progressed to a location within the penumbra with a similar ‘critical’ cerebral blood flow value of about 35% of control values. Since the cerebral blood flow gradient is linear in all of these simulations, increasing the size of the initial lesion core or of the penumbra effectively assigns the critical blood flow value to a cortical element that is farther out along the penumbra. The net effect is an increase in the number of cortical elements that become infarcted.

*Figures 4 and 5 go here*

Figure 5 plots the duration of elevated extra-cellular potassium levels (defined as the time required for potassium levels to begin falling monotonically to basal levels, e.g., at roughly 1.2 hours in Figure 2a) in the lesion core versus the number of CSD waves in simulations which yielded 1 to 7 waves. A highly significant linear correlation was found, and represents a testable prediction of the model.

We also examined the physical characteristics of CSD waves as they propagate across the penumbra. There was a trend towards an increase in the velocity (up to 11 %) at the distal edge of the penumbra compared to CSD waves measurements near mid-penumbra and a decrease in the duration (up to 28 % at the distal edge compared to near mid-penumbra) of CSD waves as they moved across the penumbra. These results are consistent with the hypothesis that CSD wave propagation is directly influenced by the metabolic status of the tissue through which it propagates. Since cerebral blood flow, metabolic stores and hemodynamic responses are graded across the penumbra, the more distal from the core center the recording site is, the larger the metabolic reserves are and the greater the degree of cerebral blood flow coupling is to metabolic demands. When the CSD waves invade the normal tissue surrounding the penumbra, the physical characteristics of the CSD waves approach values found in the normoxic simulations.

#### **2.4 Effects of Mid-Penumbra Cerebral Blood Flow and Potassium Reuptake Rate**

To further show that the parameter set we use is an adequate one, i.e., that it generates a model whose behavior is in close correspondence with experimental data, we conducted two experiments investigating the effects of mid-penumbra cerebral blood flow levels and potassium reuptake rate on

the final infarct size. The potassium reuptake rate reduces extracellular  $K^+$  levels in a metabolic energy dependent manner, and we therefore equate this variable with the membrane Na/K-ATPase activity of neurons and/or glia.

*Figure 6 goes here*

The model exhibits an inverse relationship between infarct volume and mid-penumbra cerebral blood flow, as shown in Figure 6a. Taking mid-penumbra flow as essentially representing mean penumbra flow, this successfully reproduces experimental results indicating an inverse relationship between the mean cerebral blood flow and final infarct volume (Takagi *et al.*, 1993). Mean cerebral blood flow, in the study by Takagi *et al.*, is defined as the average cerebral blood flow over time, measured at a single location, during middle cerebral artery occlusion, expressed as a percentage of pre-occlusion cerebral blood flow levels. In the model, the cerebral blood flow at a particular cortical element is constant over time, except when a CSD wave passes through the cortical element. To generate different mid-penumbra values for comparison, we created penumbræ with various non-linear cerebral blood flow gradients and placed the recording electrode half way into the penumbra.

Figure 6b plots the final infarct area versus the parameter  $c_{RK}$ , which directly modulates the potassium reuptake rate. The inverse relationship found in the model between final infarct area and the parameter  $c_{RK}$  (corresponding to Na/K-ATPase activity) is consistent with experimental results (Williams *et al.*, 1994). In addition to decreasing the final infarct area, an increase in the parameter  $c_{RK}$  also reduced the duration and the number of CSD waves compared to a simulation with a smaller value for this parameter. Interestingly, the total expenditure of metabolic energy is actually reduced when  $c_{RK}$  is increased because of the reduction in the duration and the number of CSD waves (data not shown). Thus, enhancing Na/K-ATPase activity may actually reduce metabolic load and tissue damage in the penumbra, suggesting a new possible therapeutic avenue for future studies.

## **2.5 Effects of Varying Model Parameters on Number of CSD Waves and Damage**

To determine which parameters control the generation of variable numbers of CSD waves, we systematically modified parameters (plus or minus one order of magnitude) relative to the base case (Table 3, in the Appendix). Table 1 shows the qualitative effects of parameter variations on

the number of ischemic CSD waves and the amount of tissue damage. A (+) indicates a positive correlation between the value of the parameter and the resulting number of CSD waves or amount of damage, a (-) indicates an inverse correlation, and  $\pm$  indicates no correlation in the number of CSD waves or damage. As the effects of such variations on ischemic strokes are largely unknown, the resulting correlations represent testable predictions of the model.

*Tables 1 and 2 go here*

The parameters that most greatly affected the number of CSD waves were  $c_{MR}$  and  $c_{RR}$  (in conjunction with  $P_{\Theta}$ ). The parameter  $c_{MR}$  determines the metabolic cost of reuptake. By increasing the cost of reuptake, the level of metabolic stores is proportionately reduced. The reduction in metabolic stores production rate increases the time required for ion equilibrium to be established and hence increases the duration of a CSD wave, which increases the amount of damage that occurs per wave. In addition, a reduction in the metabolic stores reduces the potassium reuptake rate ( $M$  directly modulates the rate of potassium reuptake), which leads to an increase in the number of CSD waves. The  $c_{RR}$  parameter effects the net rate at which potassium reuptake occurs. With a slower reuptake rate, the probability of a CSD wave occurring is increased. For a CSD wave to occur, extracellular  $K^+$  levels must exceed a threshold value ( $K_{\Theta}$  in the model). The probability of this occurring depends directly on the ability of the cortical elements to reuptake extracellular  $K^+$ . Any reduction in the rate of this process will increase the likelihood that a CSD wave is generated. In addition, the duration of a CSD wave is prolonged with a slower reuptake rate, which again increases the amount of damage incurred per wave. In addition to these two parameters, Table 2 lists the values for  $P_{\Theta}$  for the simulations that produced multiple CSD waves plotted in Figure 3a.  $P_{\Theta}$  alone does not positively correlate with the number of CSD waves *and* the amount of damage (see Table 1). However, when this parameter was varied (lowered) in conjunction with  $c_{MR}$  and  $c_{RR}$ , fewer CSD waves could be obtained.

There are three parameters listed in Table 1 that reduce both the number of CSD waves and the resulting damage ( $c_{FM}$ ,  $c_{RK}$ , and  $c_{SS}$ ). The parameter  $c_{FM}$  regulates the rate at which cerebral blood flow responds when metabolic stores production changes. An increase in this parameter allows a tighter coupling between cerebral blood flow and metabolic stores production. The greater the degree of coupling between these two variables, the less likely the metabolic stores level will allow metabolic stores to drop below the intactness threshold. The parameter  $c_{RK}$  has a direct impact

on the activity of the reuptake process and it is not remarkable that increasing the magnitude of reuptake activity will reduce the number and the duration of CSD waves. The fact that it also reduces the damage reflects the effect of CSD wave duration on tissue damage: increased wave duration increases tissue damage. The parameter  $c_{SS}$  directly modulates the rate of potassium release from the internal stores when infarction occurs. If potassium leakage from infarcted tissue occurs quickly, the stimulus for CSD waves will be reduced.

Lastly, the results from the model are not critically dependent upon a spatially uniform set of values for the parameters and constants employed in the model. We repeated the base experiments that generated multiple CSD waves, while randomly changing the local values of parameters that generated controllable numbers of CSD waves (see Table 2). Spatial variation of parameters was accomplished by allowing their magnitude to fluctuate around their mean reference values. Fluctuations up to  $\pm 25\%$  of their reference value did not alter qualitatively the physical characteristics (i.e. velocity and duration) of the CSD waves, an indication of the robustness of our results.

### 3 Discussion

This paper presents the first computational model examining the hypothesized role of CSD waves in ischemic stroke. As discussed earlier, previous computer models related to CSD have been limited to normoxic CSD waves, and have focused mainly on studying ionic changes and the generation of such waves; none have been used to study ischemic depolarizations. Conversely, previous computational studies of stroke have all concentrated on the study of the reorganization of cortical maps following focal lesions (Sutton *et al.*, 1994; Xing & Gerstein, 1996; Goodall *et al.*, 1997). These models focus on neural activity and connectivity, and do not encompass any of the metabolic and pathophysiological changes that accompany acute stroke.

The idea of using computational models to study neurological diseases is not new. During the last several years models of Alzheimer’s disease, epilepsy, aphasia, acquired dyslexia, Parkinsonism, migraine aura, and other disorders have been studied to obtain a better understanding of the underlying pathophysiological processes (Reggia *et al.*, 1996). The complexity of the events in stroke suggests that computational models can also be powerful tools for its investigation. While computer models have the disadvantage of simplifying the underlying neurobiology and the pathophysiology of stroke, they permit precise and systematic control of the lesion size/location and allow an arbitrarily

large number of “subjects.” They are open to detailed inspection, in isolation, of the influence of various metabolic and neural variables on infarct progression, in the hope of gaining insight into *why* observed behaviors occur.

Our results show that the basic formulation developed previously for the computational study of normoxic CSD waves can be extended in a natural, straightforward manner to study ischemic CSD. Our model generates CSD waves that have similar characteristics to those observed experimentally, regarding their form, velocity, and duration (Mies *et al.*, 1991). Under the constraint that the basic parameter values that characterize CSD dynamics and generation in the ischemic case should be essentially similar to those used in the normoxic case, the extended model developed here is used to study CSD generation in stroke by altering the blood supply to cortical tissue. As shown, our model can successfully reproduce the general form and properties of CSD waves in the ischemic penumbra, and the typical profiles of blood flow response and increasing metabolic shortage observed in animal models of ischemic CSD.

The model has been used to conduct several simulation experiments that examine the plausibility of the hypothesis that CSD waves increase infarct volume from a computational perspective. Our findings may be summarized as follows:

1. The model displays the strong linear correlation found between the number of CSD waves traversing the penumbra and final infarct size. It explains how this overall linear correlation is observed while the damage observed in each individual acute stroke experiment progresses sub-linearly over time.
2. The model successfully reproduces the experimental dependency of final infarct size on mean cerebral blood flow and Na/K-ATPase levels (the latter represented by  $R$  in the model).
3. Detailed quantitative predictions are generated, describing the effects of the initial infarct size and the extent of the accompanying penumbra on the final infarct size. A ‘critical’ penumbra blood flow level is identified, beyond which damage does not progress.
4. Several testable predictions characterizing ischemic CSD waves in the penumbra are made:
  - A. The number of CSD waves generated by the model is highly correlated with the duration of elevated potassium in the infarct core.
  - B. The velocity of CSD waves is dependent on the metabolic energy reserves of the tissue; it should increase as the wave spreads along the

penumbra, approaching the velocity found in the normoxic case when it reaches the perfused tissue surrounding the penumbra. C. The duration of ischemic CSD waves is contingent upon the recording location, and should decrease as the wave traverses the penumbra. These predictions could be tested by measurements along multiple sites within the infarct core, the penumbra and its surrounding.

5. A preliminary parameter search has been made in order to identify the effects of model parameters on CSD generation and resulting tissue damage. A more extensive and systematic parameter search is needed in order to identify possible candidates for therapeutic intervention.

These findings support the likelihood that CSD waves may play an important causal role in the progression of penumbra tissue damage. They gain further validity in light of the demonstrated robustness of the model to significant random fluctuations in the parameter values of individual cortical elements around the mean values defined in our reference parameter set (Table 3, Appendix).

The model presented in this paper lays the foundations for further computational study of acute focal stroke and the ischemic penumbra. Making some first steps in this investigation, we have chosen to focus on a minimal set of variables that could provide meaningful insight as to the role of CSD waves in the penumbra. To develop the model further, some important limitations of the model should be addressed. Additional variables that are known to play a significant role in the penumbra, such as calcium ions and glutamate, should be added. This would allow the computational study of possible ways for enhancing the therapeutic efficacy of calcium blockers and NMDA antagonists in reducing penumbra damage. In addition, further exploration of the parameter space is needed. So far, the choice of parameter values has been guided by two main kinds of constraints: the need to generate normoxic and ischemic CSD waves with characteristics that fit the relevant experimental data, and the need to obtain a model with spatial and temporal scales that are adequate for the description of acute focal stroke, which in small animal models takes place over a few centimeters of cortex during a few hours. The parameter setting task has been successfully achieved via an arduous search process. However, we do not know if this set of parameters is unique, i.e., if it is the only set that generates a behavior consistent with the experimental constraints.

The experimental finding of a linear correlation between the number of CSD waves and the

extent of penumbra tissue death has rejuvenated interest in the study of CSD waves because of its potential causal role. While our results bring support to the hypothesis that CSD waves have a causal role in penumbra tissue death (and generate some testable quantitative predictions concerning the effects of various variables on the final infarct size), the possibility that penumbra damage is caused by other metabolic causes has, of course, not been excluded.

Finally, from a broader perspective, an important result of this work is the demonstration that, with recent developments in the computational power available, a complex multi-variate computational study of acute stroke has now become a feasible task. While this and previous studies are just first steps in investigating stroke with formal computational modeling tools, we feel that they demonstrate that this task is feasible.

## Appendix: Model Description

In the following equations, variables are denoted by a single capital letter (e.g.,  $K$ ,  $R$ ), constant parameters by subscripts to the variables' names (e.g.,  $K_{rest}$ ,  $M_\theta$ ), and multiplicative constants begin with a lower case "c" which is subscripted by two capital letters, both of which are usually names of variables. The first letter is the name of the variable whose equation contains this constant, and the second letter is usually the name of a variable that the constant modulates (e.g.,  $c_{KS}$  is the constant associated with the effect on the external potassium  $K$  of the internal potassium stores  $S$ ). Numerical values for all parameters used in the simulations presented in this paper are listed in Table 3 at the end of this appendix.

Both the spatial structure of the cerebral cortex and time are discretized. The cortex is represented as a two-dimensional array of elements, each of which represents a small volume of cortex. A hexagonal tessellation of the cortex is assumed, so each element has six immediately adjacent neighbor elements. Each cortical element  $i$  has its own value for extracellular potassium  $K_i$ , reuptake  $R_i$ , metabolic stores  $M_i$ , persistent impairment  $P_i$ , intactness  $I_i$ , internal potassium stores  $S_i$ , and cerebral blood flow  $F_i$ , governed by the equations below.

The rate of change of extracellular potassium concentration  $K_i(t)$  of element  $i$  at time  $t$  is governed by the reaction-diffusion equation

$$\frac{\partial K_i}{\partial t} = c_{KA}(K_i - K_{rest})(K_i - K_\theta)(K_i - K_{max})(K_i + 0.1)I_i + c_{KS}(S_i - I_i)(K_{max} - K_i) - K_i R_i + c_{KD} \nabla K_i + K_{inf} \quad (1)$$

where  $c_{KA} < 0$ ;  $K_{rest}$ ,  $K_\theta$ ,  $K_{max}$ ,  $c_{KS}$ ,  $c_{KD} > 0$ ;  $K_{inf} \geq 0$  are constants. Initially,  $K_i = K_{rest}$  for all elements. The first term, the reaction term, meets the following requirements: homeostatic maintenance of resting extracellular potassium level  $K_{rest}$  (approx. 3 mM in the cortex), a threshold  $K_\theta > K_{rest}$  beyond which elevated  $K_i$  triggers explosive subsequent growth in  $K_i$ , and a ceiling  $K_{max} > K_\theta$  above which  $K_i$  does not rise. As these dynamics require normal mechanisms operative in undamaged tissue, this term is multiplied by the level of cortical intactness,  $I_i$ . The second term represents the pathological leakage of intracellular potassium into the extracellular space in damaged, infarcted tissue. It is a function of the levels of intracellular potassium stores  $S_i$ , tissue intactness  $I_i$ , and extracellular potassium. The third term reflects reuptake of potassium. The fourth term represents diffusion of  $K^+$  through the cortex, where  $c_{KD}$  is the potassium diffusion coefficient and  $\nabla^2$  is the Laplacian operator. In order to implement the discrete form of the Lapla-

cian operator, we multiplied the extracellular  $K_i$  level for element  $i$  by the number of neighboring elements and subtracted from this value the sum of the extracellular  $K$  values of these neighbors. The last term,  $K_{inf}$ , represents external infusion of  $K^+$  into the simulated cortex. In the normoxic simulations,  $K_{inf}$  is set to a small positive value for those cortical elements in a  $5.17 \text{ mm}^2$  area (i.e., equal in area to the initial lesion core in the ischemic simulations) for 5 minute intervals.

The rate of potassium reuptake,  $R_i$ , reflecting the functioning of membrane bound Na/K pumps, is modeled by

$$\frac{dR_i}{dt} = c_{RK}(P_\theta - P_i)I_iM_i(K_i - K_{rest}) - c_{RR}(K_{max} - K_i + c_R)R_i \quad (2)$$

The first term reflects reuptake proportional to the levels of partial impairment, tissue intactness, and extracellular potassium and the second is a decay term, which contains extracellular potassium-dependent and independent components. The initial value of  $R_i$  is 0.

The metabolic stores that determine the energy status of the tissue, such as glucose, and the high energy phosphate pool, are grouped together in a single variable  $M_i$ , and are governed by

$$\frac{dM_i}{dt} = c_{MF}F_iI_i(P_\theta - P_i)(M_t - M_i) - (c_{MR}R_i + c_{MM})M_i \quad (3)$$

where  $c_{MF}, M_t, c_{MR}, c_{MM} > 0$  are constants.  $M_t$  is the equilibrium level of metabolic stores.  $c_{MM}$  is the basal level of energy expenditure. Initially,  $M_i$  starts at  $M_{rest}$ . The first term in equation (3) is a supply term, proportional to blood flow and tissue intactness levels, and inversely related to metabolic stores production rate.  $P_i$  is the partial impairment of element  $i$ , and the addition of the factor  $(P_\theta - P_i)$  to the supply term incorporates the reduced ability of an impaired element to extract metabolic building blocks from the blood. The second term represent the metabolic load imposed by potassium reuptake and the basic metabolic rate.

The partial impairment variable  $P_i$  represents stresses on element  $i$  that compromise its integrity, such as decreased pH, increase in intracellular  $Ca^{2+}$ , etc. When the metabolic stores  $M_i$  drop below the partial impairment threshold ( $M_\Theta$ ), the partial impairment for cortical element  $i$  increases in proportion to the magnitude of the difference between  $M_\Theta$  and  $M_i$ .

$$\frac{dP_i}{dt} = c_{PP}(M_\Theta - M_i)I_i \quad (4)$$

where  $c_{PP} > 0$  is a constant.  $P_i$  remains unchanged when  $M_i > M_\Theta$ , and the initial value for  $P_i$  is 0.

Penumbra cerebral blood flow is regulated by

$$\frac{dF_i}{dt} = c_{FM}(M_{rest} - M_i)(F_{max} - F_i)I_i + c_{FF}(F_{max}/2 - F_i) \quad (5)$$

where  $c_{FM}, M_{rest}, F_{max}, c_{FF} > 0$  are constants and  $c_{FM} > c_{FF}$ .  $M_{rest}$  is the initial metabolic stores level,  $F_{max}$  is the absolute ceiling for the blood flow rate and  $F_{max}/2$  is the equilibrium rate of blood flow in normal tissue. Initially,  $F_i$  is  $F_{max}/2$ . The first term in (5) represents the dependency of blood supply on the status of the metabolic stores and current blood flow levels. The second term self-regulates blood flow towards its basal rate.

Variable  $I_i$  is an indicator of the intactness of element  $i$ , identifying the fraction of the element that is undamaged. Damage, which is assumed irreversible, occurs only below a critical metabolic threshold level  $M_i < (P_\theta + P_i)$ , and is proportional to this energy deficiency,

$$\frac{dI_i}{dt} = c_{II}(M_i - (P_\theta + P_i))I_i \quad (6)$$

where  $c_{II}, P_\theta > 0$  are constants.  $I_i$  remains unchanged when  $M_i \geq (P_\theta + P_i)$ , and initially,  $I_i$  is 1.0. This threshold for tissue intactness is directly dependent on the persistent impairment  $P_i$ .

The leakage of potassium from intracellular to the extracellular space occurs when the intactness for a given cortical element,  $I_i$ , begins to drop. This formulation is expressed in the following equation,

$$\frac{dS_i}{dt} = c_{SS}(I_i - S_i) \quad (7)$$

where  $c_{SS} > 0$  is a constant. Initially,  $S_i$  starts at 1.0.

Boundary conditions are set along the edges of the simulated cortex. The results are similar with leakage and sealed-end boundary conditions. In both cases, when CSD waves reach the edge of the simulated cortex, they dissipate immediately. This is consistent with numerous reports (Grafstein, 1956a; Grafstein, 1956b; Bures *et al.*, 1974) indicating that CSD waves do not propagate across sulci. Since we have not included sulci in the present version of the model, these boundary conditions provide a functional equivalence to sulci with respect to CSD wave propagation properties.

In order to calculate the duration and velocity of CSD waves in the model, the temporal and spatial characteristics of the simulated cortex is required. The value of one time unit (tick, or iteration) in the program is given by

$$tick\ scale = literature\ duration / simulation\ duration$$

where ‘literature duration’ (‘simulation duration’) denotes the duration of a CSD wave reported experimentally (measured in the simulation), respectively. The duration of a CSD wave in the model is determined as the number of program iterations which elapse while  $K^+$  is above 0.5. The “literature” duration is taken to be 80 seconds for normoxic CSD waves. The length of one spatial unit in the model (‘cell scale’) is given by

$$cell\ scale = (literature\ velocity / simulation\ velocity) \cdot tick\ scale$$

where ‘literature (simulation) velocity’ denotes the CSD wave velocity reported experimentally (measured in the simulation), respectively. The simulation velocity is given as the number of units (cells) that the wave traverses in a given time unit. The “literature” velocity is taken to be 4.8 mm/min for normoxic CSD waves. Substituting values reported in the literature for CSD wave duration and velocity yields 0.125 mm as the cell scale and 13 msec ( $2.167 * 10^{-4}$  min) as the tick scale, the program time-step.

*Table 3 goes here*

## References

- Back, T., Kohno, K., & Hossmann, K.A. (1994). Cortical negative DC deflections following middle cerebral artery occlusion and KCL-induced spreading depression: Effect on blood flow, Tissue oxygenation, and electroencephalogram. *Journal of Cerebral Blood Flow and Metabolism*, **14**, 12–19.
- Back, T., Zhao, W., & Ginsberg, M. D. (1995). Three-dimensional image analysis of brain glucose metabolism - blood flow uncoupling and its electrophysiological correlates in the acute ischemic penumbra following middle cerebral artery occlusion. *Journal of Cerebral Blood Flow and Metabolism*, **15**, 566–577.
- Back, T., Ginsberg, M. D., Dietrich, W.D., & Watson, B.D. (1996). Induction of spreading depression in the ischemic hemisphere following experimental middle cerebral artery occlusion: effect on infarct morphology. *Journal of Cerebral Blood Flow and Metabolism*, **16**(2), 202–213.
- Bures, J., Buresova, O., & Krivanek, J. (1974). *The Mechanism and Application of Leao's Spreading Depression of Electroencephalographic Activity*. Academic Press, Inc. Chap. 1.
- Cheer, A., Nuccitelli, R., Oster, G.F., & Vincent, J.P. (1987). Cortical activity in vertebrate eggs I: The activation waves. *Journal of Theoretical Biology*, **124**, 377–404.
- Chen, Q., Chopp, M., Bodzin, G., & Chen, H. (1993). Temperature modulation of cerebral depolarization during focal cerebral ischemia in rats: correlation with ischemic injury. *Journal of Cerebral Blood Flow and Metabolism*, **13**, 389–394.
- Choi, D.W. (1994). Glutamate receptors and the induction of excitotoxic neuronal death. *Progress in Brain Research*, **100**, 47–51.
- Fisher, M., & Garcia, J. (1996). Evolving stroke and the ischemic penumbra. *Neurology*, **47**(October), 884–888.
- FitzHugh, R. (1961). Impulses and physiological states in theoretical models of nerve membrane. *Biophysics Journal*, **1**, 445–466.
- Gault, L.M., Lin, C.W., LaManna, J. C., & Lust, W.D. (1994). Changes in energy metabolites, cGMP and intracellular pH during cortical spreading depression. *Brain Research*, **641**, 176–180.
- Gill, R., Andine, P., Hillered, L., Persson, L., & Hagberg, H. (1992). The effect of MK-801 on cortical spreading depression in the penumbral zone following focal ischemia in the rat. *Journal of Cerebral Blood Flow and Metabolism*, **12**, 371–379.

- Goodall, S., Reggia, J.A., Chen, Y., Ruppin, E., & Whitney, C. (1997). A computational model of acute focal cortical lesions. *Stroke*. in Press.
- Gorelova, N., Krivanek, J., & Bures, J. (1987). Functional and metabolic correlates of long series of cortical spreading depression waves in rat. *Brain Research*, **404**, 379–381.
- Grafstein, B. (1956a). Locus of propagation of spreading cortical depression. *Journal of Neurophysiology*, **19**, 308–315.
- Grafstein, B. (1956b). Mechanism of spreading cortical depression. *Journal of Neurophysiology*, **19**, 154–171.
- Gyngell, M., Back, T., & Hoehn-Berlage, M. (1994). Transient cell depolarization after permanent middle cerebral occlusion: and observation by diffuse-weighted MRI and localized 1H-MRS. *Magnetic Resonance in Medicine*, **31**, 337–341.
- Hansen, A.J., & Mutch, W.A.C. (1984). Water and ion fluxes in cerebral ischemia. *Pages 121–130 of: Siesjo, B.K. (ed), Cerebral Ischemia*. Excerpta Medica.
- Hansen, A.J., Quistorff, B., & Gjedde, A. (1980). Relationship between local changes in cortical; blood flow and extracellular potassium during spreading depression. *Acta Physiol. Scand*, **109**, 1–6.
- Heiss, W.D., & Graf, R. (1994). The ischemic penumbra. *Current Opinion in Neurology*, **7**, 11–19.
- Hossman, K.A. (1994a). Viability thresholds and the penumbra of focal ischemia. *Annals of Neurology*, **36**, 557–565.
- Hossmann, K.A. (1994b). Glutamate-mediated injury in focal cerebral ischemia: The excitotoxin hypothesis revised. *Brain Pathology*, **4**, 23–36.
- Iijima, T., Meis, G., & Hossmann, K.A. (1992). Repeated negative deflections in rat cortex following middle cerebral artery occlusion are abolished by MK-801. Effect on volume of ischemic injury. *Journal of Cerebral Blood Flow and Metabolism*, **12**, 727–733.
- Lane, D.C., Murray, J.D., & Manoranjan, V.S. (1987). Analysis of wave phenomena in a morphogenetic mechanochemical model and an application to post-fertilisation waves on eggs. *IMA J. Math. Appl. Med. Biol.*, **4**, 309–331.
- Lauritzen, M. (1994). Pathophysiology of the migraine aura: The spreading depression theory. *Brain*, **117**, 199–210.
- Mayevsky, A., & Weiss, H.R. (1991). Cerebral blood flow and oxygen consumption in cortical spreading depression. *Journal of Cerebral Blood Flow and Metabolism*, **11**, 829–836.

- Mayevsky, A., Zarchin, N., & Friedli, C.M. (1982). Factors affecting the oxygen balance in the awake cerebral cortex exposed to spreading depression. *Brain Research*, **236**, 93–105.
- Mies, G., & Paschen, W. (1984). Regional changes of blood flow, glucose and ATP content determined on brain sections during a single passage of spreading depression in rat brain cortex. *Experimental Neurology*, **84**, 249–258.
- Mies, G., Iijima, T., & Hossmann, K.A. (1993). Correlation between peri-infarct DC shifts and ischaemic neuronal damage in rat. *Neuroreport*, **4**, 709–711.
- Mies, G. M., K., Y. Xie, Seo, & Hossman, K.-A. (1991). Ischemic thresholds of cerebral protein synthesis and energy state following middle cerebral artery occlusion in rat. *Journal of Cerebral Blood Flow and Metabolism*, **11**, 753–761.
- Nagumo, J., Arimoto, S., & Yoshizawa, S. (1962). An active pulse transmission line simulating nerve axon. *Proc. IRE*, **50**, 2061–2071.
- Nedergaard, M., & Astrup, J. (1986). Infarct rim: effect of hyperglycemia on direct current potential and 2-deoxyglucose phosphorylation. *Journal of Cerebral Blood Flow and Metabolism*, **6**, 607–615.
- Nedergaard, M., & Hansen, A.J. (1988). Spreading depression is not associated with neuronal injury in the normal brain. *Brain Research*, **449**, 395–398.
- Nedergaard, M., & Hansen, A.J. (1993). Characterization of cortical depolarizations evoked in focal cerebral ischemia. *Journal of Cerebral Blood Flow and Metabolism*, **13**, 568–574.
- Pulsinelli, W. (1992). Pathophysiology of acute ischaemic stroke. *The Lancet*, **339**, 533–536.
- Reggia, J., & Montgomery, D. (1996). A computational model of visual hallucinations in migraine. *Computers in Biology and Medicine*, **26**(2), 133–141.
- Reggia, J., E. Ruppin, & Berndt, R. (eds), (1996). *Neural Modeling of Brain and Cognitive Disorders*. United Kingdom: World Scientific Publishing.
- Reith, W., Hasegawa, Y., Latour, L.L., Dardzinsli, B.J., Sotak, C.H., & Fisher, M. (1995). Multi-slice diffusion mapping for 3-D evolution of cerebral ischemia in a rat stroke model. *Neurology*, **45**, 172–177.
- Reshodko, L.V., & Bures, J. (1975). Computer simulation of reverberating spreading depression in a network of cell automata. *Biol. Cybernetics*, **18**, 181–189.
- Sugaya, E., Takato, M., & Noda, Y. (1975). Neuronal and glial activity during spreading depression in cerebral cortex of cat. *J. Neurophysiology*, **38**, 822–841.

- Sutton, G., Reggia, J., & Armentrout, S. (1994). Cortical map formation as a competitive process. *Neural Comp*, **6**, 1–13.
- Takagi, K., Ginsberg, M. D., Globus, M.Y., Dietrich, W.D., Martinez, E., S.Kraydieh, & Busto, R. (1993). Changes in amino acid neurotransmitters and cerebral blood flow in the ischemic penumbral region following middle cerebral artery occlusion in the rat: correlation with histopathology. *Journal of Cerebral Blood Flow and Metabolism*, **13**, 575–585.
- Takano, K., Latour, L.L., Formato, J.E., Carano, R.A.D., Helmer, K.G., Hasegawa, Y., Sotak, C., & Fisher, M. (1996). The role of spreading depression in focal ischemia evaluated by diffusion mapping. *Annals of Neurology*, **39**, 308–318.
- Tuckwell, H.C., & Miura, R.M. (1978). A mathematical model for spreading cortical depression. *Biophysical Journal*, **23**, 257–276.
- Williams, G. D., Towfighi, J., & Smith, M. B. (1994). Cerebral energy metabolism during hypoxia-ischemia correlates with brain damage: a  $^{31}\text{P}$  NMR study in unanesthetized immature rats. *Neuroscience Letters*, **170**, 31–34.
- Xing, J., & Gerstein, G. (1996). Networks with lateral connectivity. *Journal of Neurophysiology*, **75**, 184–232.
- Zhang, Z. G., Chopp, M., Maynard, K. I., & Moskowitz, M. A. (1994). Cerebral blood flow changes during cortical spreading depression are not altered by inhibition of nitric oxide synthesis. *Journal of Cerebral Blood Flow and Metabolism*, **14**(6), 939–943.

## Captions

Figure 1: Simulation results from approximately 2 hours of intermittent application of 150 units of  $K^+$  applied to a central region of the simulated normoxic cortex. The horizontal axis represents time in hours and the vertical axis represents the magnitude of the corresponding variables used in the model, measured 5.75 mm from the stimulus center. The variables plotted are: K (extracellular potassium levels), R (potassium reuptake rate), M (metabolic stores level), and F (cerebral blood flow).

Figure 2: Ischemic CSD simulation. a) Recordings from the infarct center when cerebral blood flow is clamped to zero for 2 hours. In addition to the variables presented in the normoxic case (Figure 1), the plots include the variables I (intactness levels), S (internal potassium stores) and P (partial impairment). The horizontal axis represents time after clamping the cerebral blood flow to zero. (b) Same as (a) but recorded from near mid-penumbra.

Figure 3: a) Cumulative infarct area versus time from onset of ischemia for four different simulations that yield 2 to 5 CSD waves respectively. The number below each line indicates the number of CSD waves that occurred during the simulation. (b) Correlation between the number of CSD waves (horizontal axis) and the final infarct area (vertical axis) for the same simulations. A linear regression line passed through these points is consistent with a very strong linear correlation ( $r = 0.992$ ,  $p < 0.005$ , linear regression line  $Y = 1.992 * X + 7.117$ ).

Figure 4: a) Final total infarct area in  $mm^2$  versus initial core lesion area in  $mm^2$ . The total ischemic area (penumbra plus lesion core) is constant with width of 7.5 mm. The relationship is close to linear ( $r = 0.973$ ,  $p < 0.003$ , linear regression line:  $Y = 0.888 * X + 6.917$ ). (b) Final total infarct area as a function of penumbra width in mm. The initial core lesion width is constant (2.5 mm). The relationship is highly linear ( $r = 0.988$ ,  $p < 0.0001$ , linear regression line:  $Y = 6.834 * X - 3.869$ ).

Figure 5: Plot of duration of elevated  $K^+$  in the lesion core (measured at the center of the lesion) versus the number of CSD waves generated. A linear regression line passed through these points, showing a very strong linear correlation ( $r = 0.988$ ,  $p < 0.0002$ , linear regression line:  $Y = 5.511 * X - 0.583$ ).

Figure 6: a) Final infarct area in  $mm^2$  versus mean cerebral blood flow at mid penumbra, expressed as a fraction of normal cerebral blood flow. The relationship is linearly correlated ( $r = -0.920$  and  $p < 0.017$ , linear regression line is:  $Y = -24.161 * X + 26.764$ ). (b) Final infarct area as a function of the parameter  $c_{RK}$ . The relationship is linearly correlated ( $r = -0.947$ ,  $p < 0.009$ , linear regression line:  $Y = -2.309 * X + 15.905$ ).

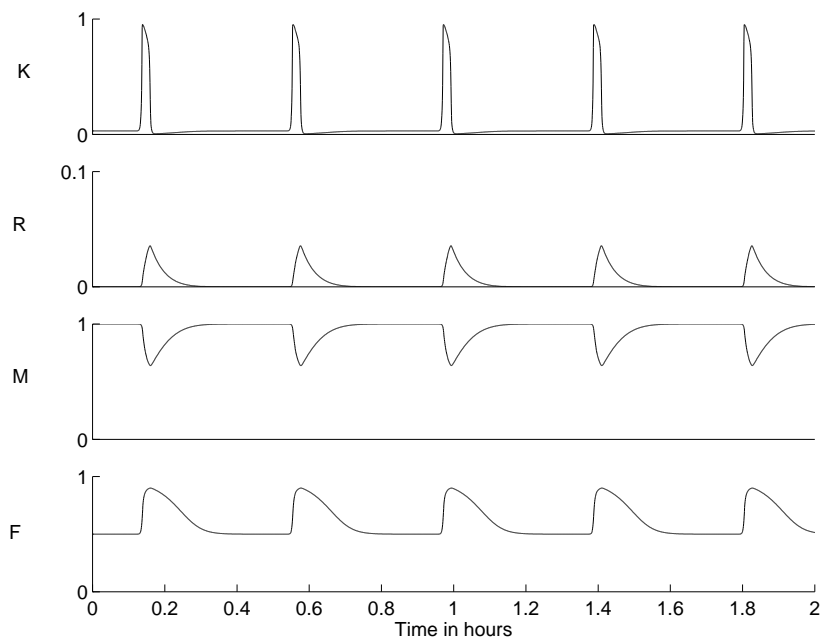
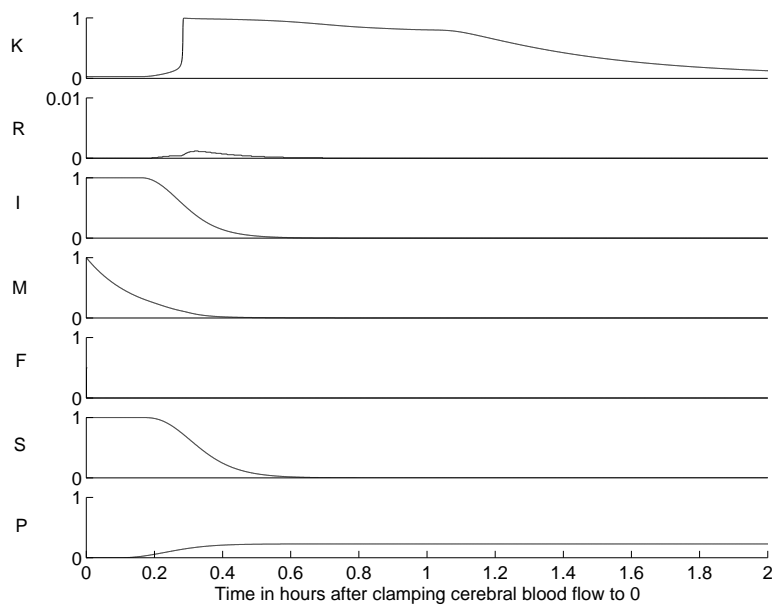


Figure 1

a)



b)

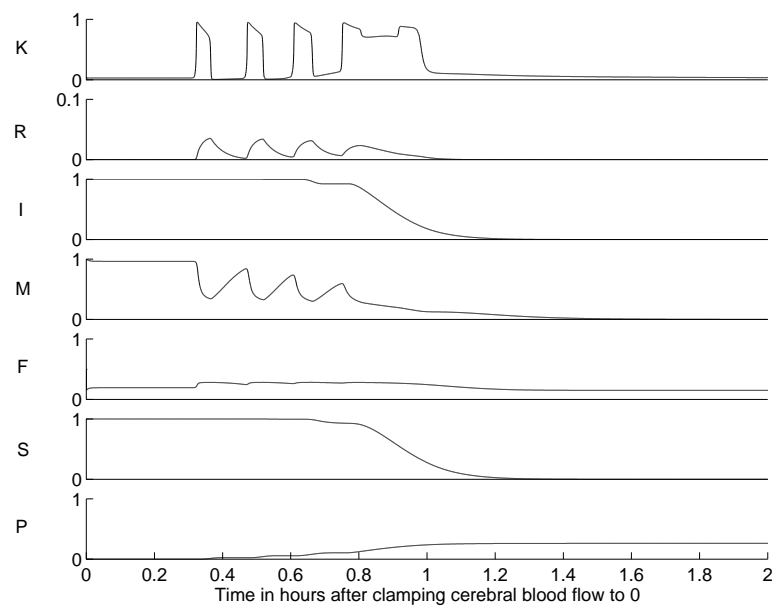
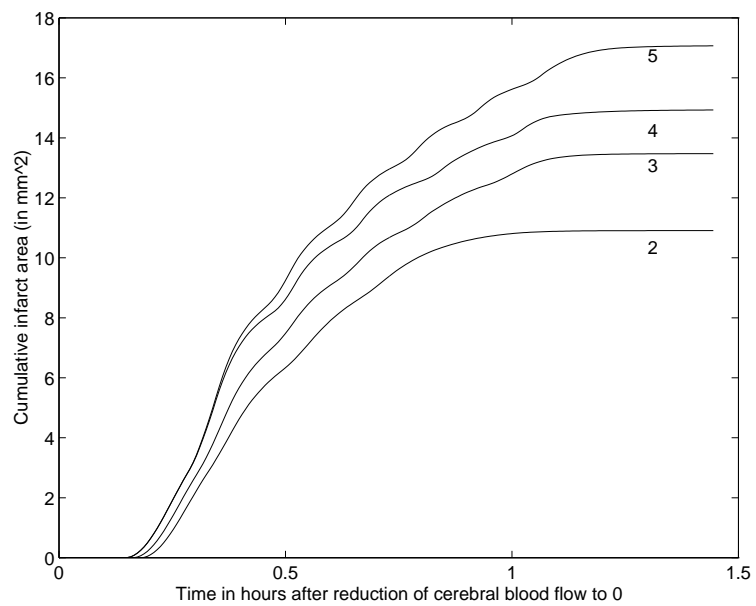


Figure 2

a)



b)

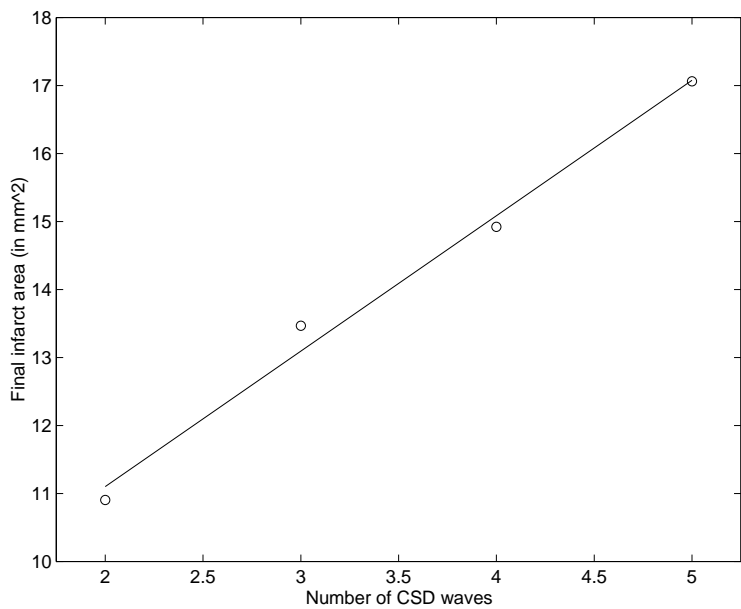
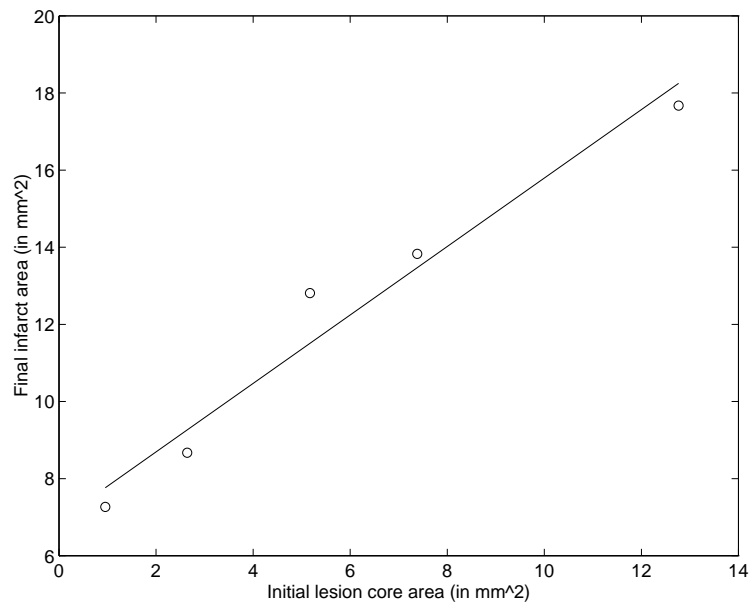


Figure 3

a.)



b.)

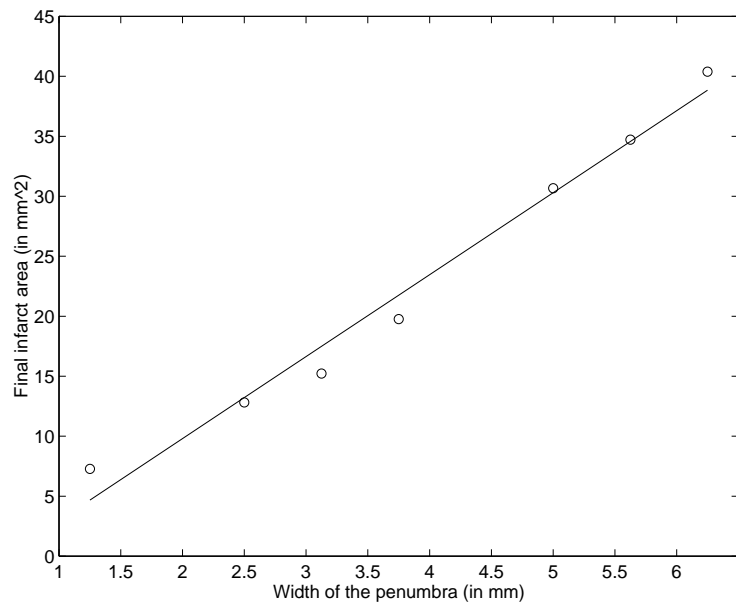


Figure 4

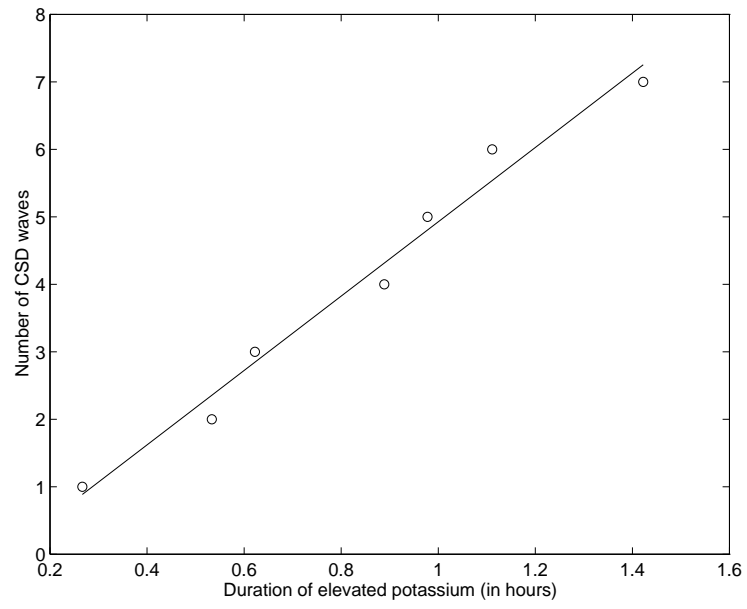
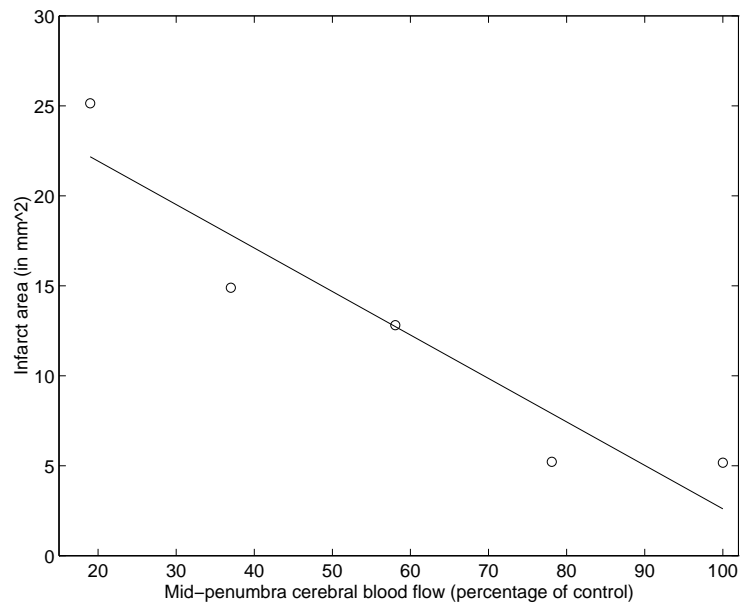


Figure 5

a)



b)

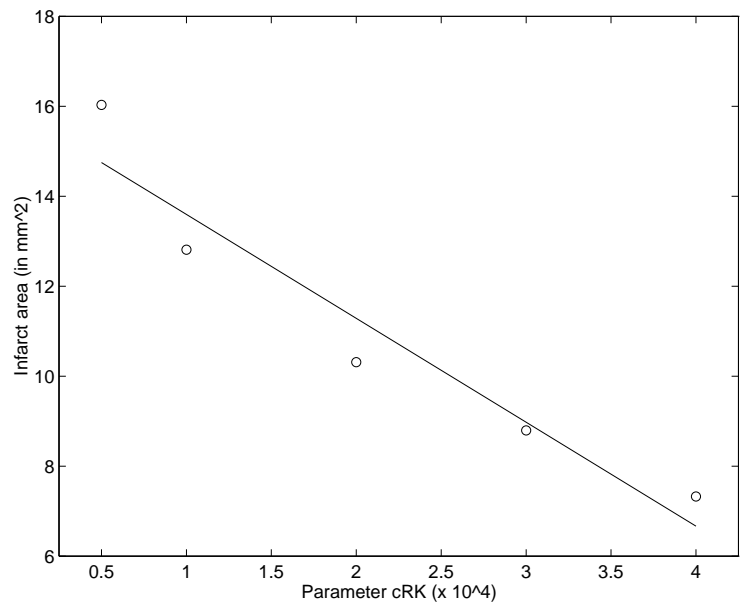


Figure 6

Table 1: Effects of parameter variations.

Parameter	Number of CSD Waves	Amount of Infarct Area
$c_{FF}$	+	$\pm$
$c_{FM}$	-	-
$M_{\Theta}$	-	+
$P_{\Theta}$	-	+
$c_{MR}$	+	+
$c_{RR}$	+	+
$c_{RK}$	-	-
$c_{KS}$	+	$\pm$
$c_{SS}$	-	-
$K_{rest}$	$\pm$	$\pm$
$c_{PP}$	$\pm$	+
$c_{II}$	$\pm$	+
$c_{KA}$	-	+

Table 2: Parameter values generating variable numbers of CSD waves

Parameter	Number of CSD waves			
	2	3	4	5
$P_{\Theta}$	0.20	0.20	0.30	0.30
$c_{MR}$	0.20	0.20	0.30	0.30
$c_{RR}$	0.000475	0.0005	0.000525	0.0006

Table 3: Reference parameter values used in the simulations.

Parameter	Ischemic Simulations	Normoxic Simulations
$K_{rest}$	0.03	0.03
$K_{\Theta}$	0.20	0.20
$K_{max}$	1.0	1.0
$c_{KD}$	0.005	0.005
$c_{KS}$	0.0035	0.0035
$c_{KA}$	-0.3	-0.3
$R_{max}$	1.00	1.0
$c_{RR}$	0.0006	0.0006
$c_{RK}$	0.00033	0.00033
$M_{rest}$	1.00	1.00
$M_{\Theta}$	0.50	0.50
$P_{\Theta}$	0.30	0.30
$M_{max}$	1.00	1.00
$c_{MF}$	0.0667	0.0667
$c_{MM}$	0.00025	0.00025
$c_{MR}$	0.30	0.30
$M_t$	$1 + 2M_{rest} * c_{MM}/c_{MF}$	$1+2M_{rest} * c_{MM}/c_{MF}$
$c_{PP}$	0.00015	0.00015
$F_{max}$	1.00	1.00
$c_{FM}$	5.00	5.00
$c_{FF}$	0.45	0.45
$c_R$	0.5	0.5
$c_{SS}$	0.001	0.001
$K_i$	0.03 ( $K_{rest}$ )	0.03 ( $K_{rest}$ )
$R_i$	0.00	0.00
$M_i$	1.0 ( $M_{rest}$ )	1.0 ( $M_{rest}$ )
$P_i$	0.0	0.0
$F_i$	Graded[0-0.5]	0.5
$I_i$	1.0	1.0
$S_i$	1.0	1.0
$c_{II}$	0.001	0.001
$K_{inf}$	0	0.0065